

Performance analysis of Pilot Mho Distance Relay for Multi-terminal Network- A review

NAEMA M. MANSOUR

Electrical Engineering Department

Suez Canal University

Ismailia

EGYPT

Abstract— The range of the possible fault current, the resistive ground fault detection, the remote infeed and directionality, the system configuration, and the heavy loaded and swing conditions are all part of the transmission line distance protection problems. In this paper, all these problems are highlighted through the analysis of the pilot distance relay performance for transmission lines with different lengths. The value of Maximum Torque Angle (MTA) and its affects on the relay sensitivity during resistive ground fault, and the minimum loadability limit of the relay and the load encroachment problem are also investigated. All these analytical studies are carried out on IEEE 9-Bus system that is modeled by MATLAB Simulink packages. Also, the relay scheme is implemented and tested using MATLAB m-code.

Index Term: Mho distance relay, IEEE 9 Bus-system, Maximum Torque Angle (MTA), load encroachment, fault resistance.

I. INTRODUCTION

Distance relay is the most widely used protective scheme for the protection of transmission, sub transmission lines, and submarine cables [1]. Comparing with over current relay, distant relay is more selective, fast, independent on the source impedance value [2-3]. However, Zone 3 of a step-distance protection relay is identified as one of the most important causes of cascading failures in power systems [4]-[6]. Distance relay is still considered one of the primary protections used for transmission line protection.

Due to its directionality feature and wide region that its characteristics covers, Mho distance relay is the most commonly used for high voltage heavily loaded transmission lines. The reach zones on the transmission line with several sections are indicated in Fig. 1. Relay at the terminal of the line is set to trip instantaneous for faults in its under-reaching Zone 1 (Z_1) that covers almost (80-90%) from the protected line, and an overreaching Zone 2 (Z_2) that covers almost (120% of the protected line) with time delay almost 15 to 30 cycles, and the backup protection Zone 3 (Z_3) that covers (220% of the protected line). Z_3 operation must be delayed to coordinate with the several Z_2 relays with almost 90 cycles time delay.

It can be noticed that distance relays provide fast protection up to 80% of the primary line length. However, the re-

maining 20% protection (that is covered by a delayed Z_2) is delayed by coordination time interval [2]. The faster fault clearing for 20% of the remote end line is needed, this can be achieved by the pilot protection distance relay.

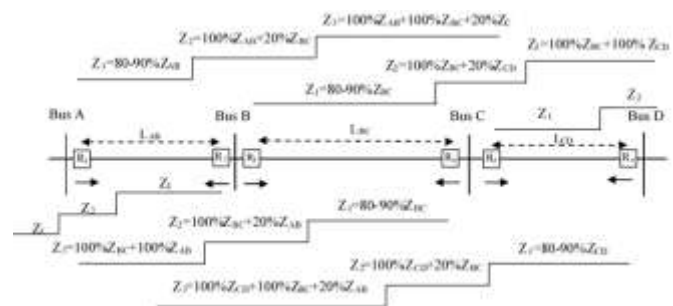


Fig. 1 Pilot wire distance relay reach zones on transmission line.

[L_{AB} , L_{BC} , L_{CD} , Z_{AB} , Z_{BC} , Z_{CD} , the line lengths and impedances of sections AB, BC, and CD respectively].

Pilot signaling is used to improve the performance of the distance protection system by initiating fast clearing on detection of faults at any portion of the protected line. In [7], a multi-terminal line configuration in many cases requires some form of pilot protection to improve speed and selectivity of the conventional distance relaying. Pilot protection is used for lines to provide the high-speed simultaneous detection of phase and ground faults for 100% of the primary line. The main idea for pilot wire relaying is to obtain the response of the distance relay element at other end to speed-up decision making.

In this paper, the performance analysis of the pilot wire Mho distance relays along the multi-sections, double infeed transmission line has been evaluated under different loading and fault conditions. To conduct this study, the modified IEEE 9-Bus system is modeled using MATLAB Simulink package. For each line section of this network, Mho distance relays are installed at its terminals. The performances of the cascaded relays are recorded and investigated. The sensitivity of all relays is tested for different faults at different locations, with different fault resistance. Also, the relays stability for external faults and different loading conditions are tested. The current and voltage signals measured at each line

section are exported to the m-code file in which the relays characteristics are implemented.

II. IEEE 9 BUS SYSTEM NETWORK

The modified IEEE 9 Bus system is simulated in this study to investigate the pilot wire distance relay performances. As in Fig. 2, the system is consisted of 3- synchronous generators(G1, G2, G3) with ratings (512, 270 and 125 MVA& 24, 18, 15.5Kv), 3- loads [(100MW, 50MVAR), (90MW, 30MVAR), (125MW, 50MVAR), and six 230KV transmission line sections with different lengths, and 9- buses. The parameters of the network are available in [9].

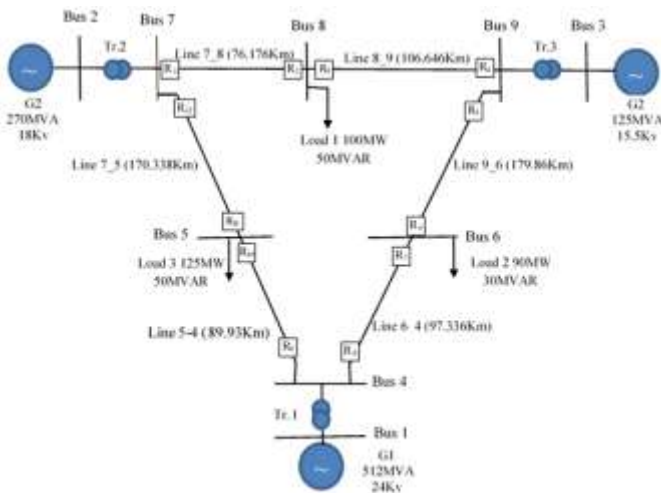


Fig. 2 Modified IEEE 9 Bus system network.

The network is simulated using MATLAB Simulink files, the load flow study and the fault analysis are carried out for all the six network sections. The output voltage and current signals are captured and exported to the m- code file.

The locations of the distance relay for each network sections are indicated in Fig. 2. The distance relay at the local and remote end of section 7-8 are $[R_1, R_2]$, and relays $[R_3, R_4]$ for section 8-9, $[R_5, R_6]$ for section 9-6, $[R_7, R_8]$ for section 6-4, $[R_9, R_{10}]$ for section 4-5, and $[R_{11}, R_{12}]$ for section 5-7. At each relay location the voltage and current measurements are installed.

III. DISTANCE MHO RELAY MODEL

Full scheme distance relays incorporates seven operating elements per zone, one for each of the phase to ground faults, one for each phase-phase fault, and one for three phase faults. The three voltage and current signals measured at the relay locations are exported to the m-code program in which the input signals that will be fed to the distance relay are calculated according to the fault types as in Table. I.

Table. I
APPERENT IMPEDANCE FORMULAS FOR DIFFERENT FAULT TYPE.

Fault type	Apparent impedance	Noting
AG	$\frac{V_a}{I_a + 3k_o I_o}$	$k_o = \frac{Z_o - Z_1}{3Z_1}$
BG	$\frac{V_b}{I_b + 3k_o I_o}$	$I_o = \frac{I_a + I_b + I_c}{3}$
CG	$\frac{V_c}{I_c + 3k_o I_o}$	k_o Residual compensation factor
AB, ABG	$\frac{V_a - V_b}{I_a - I_b}$	Z_o Zero sequence impedance of the T. L
BC, BCG	$\frac{V_b - V_c}{I_b - I_c}$	Z_1 Positive sequence impedance of the T. L
CA, CAG	$\frac{V_c - V_a}{I_c - I_a}$	I_o Zero sequence current.
ABC, ABCG	$\frac{V_a}{I_a}, \frac{V_b}{I_b}, \frac{V_c}{I_c}$	A, B, C phase A & B & C
MTA	$\tan^{-1}(X_L/R_L)$	X_L & R_L reactance and resistance of line section.

Also, the Mho distance relay characteristics are implemented based on the line section parameters. The two sections between G₂ and G₃ of the network shown in Fig. 2 is taken as example. The reach of three zones of each relay (R_1, R_2, R_3, R_4) and its directions are summarized in Fig. 3. The calculated impedances for each fault types are compared with the relay setting zones to differentiate between the faulted and non-faulted cases. Mho distance relay flowchart that summarize the relay mathematical procedure is indicated in Fig. 4. 12 Mho distance relays for the six-line sections of the tested network are implemented and tested for different fault types. Implementation of digital Mho distance relay are introduced in many publications as in [10]-[14].

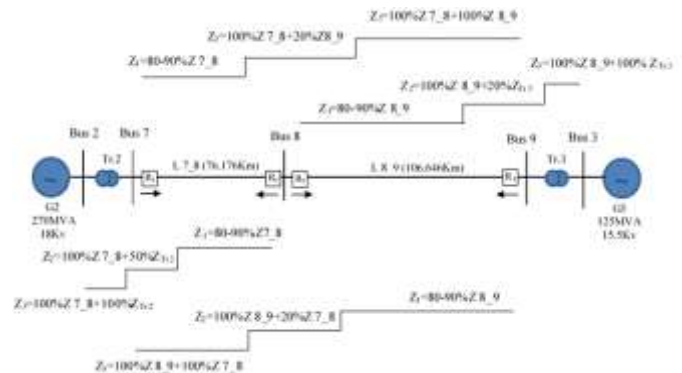


Fig. 3 Setting three zones of Mho distance relays for Section 7-8 and 8-9.

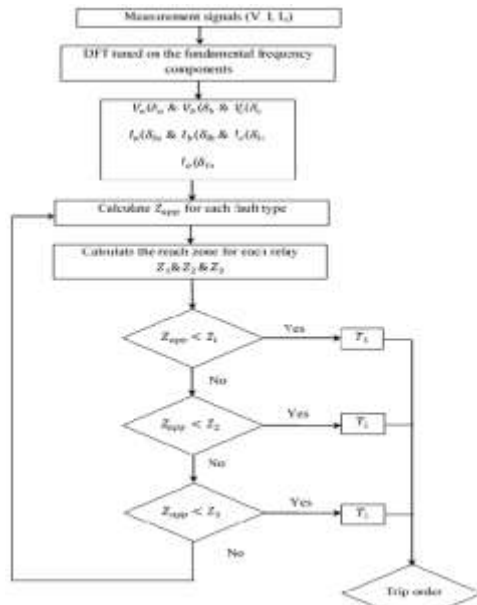


Fig.4 Implemented Mho distance relay flowchart.

IV. PILOT WIRE DISTANCE RELAY

To achieve fast tripping for all transmission line faults, the use of communication-assisted protective relaying should be considered. However, installation of communication equipment with the traditional relay schemes is much costly, but with the advancement of communications, smart measurements, and microprocessor-based relays, the cost is no longer significant issue. Moreover, the benefits of, pilot protection such as high-speed reclosing, improved system stability and power quality, easier coordination, and better resistive coverage[8].

Distance protection schemes, interfaced with communication equipment, send and receive logic-based information between relay terminals to determine if the fault is external or internal to the protected line section. Since distance relays are directional relays, the corresponding schemes are known as directional comparison schemes. The directional comparison schemes that are commonly nowadays in use are directional comparison blocking, directional comparison unblocking, overreaching transfer trip, under reaching transfer trip (non-permissive- permissive). The basic idea behind all these schemes is to obtain the response of the distance relay element at the remote end to speed- up the decision making at local end and vice versa [7]-[8].

In [7], from the considerations that recommended to take into account when determining the number of pilot systems required for the network is the voltage level. The line with voltage level from 69kV to 161kV may be or may be not provided by a pilot system. From 230kV to 345kV, there is normally at least one pilot scheme and often, depending on system configuration. Above 345kV, it is typical to apply at least two pilot schemes and direct transfer trip for equipment failure. IEEE 9-Bus system with its voltage level 230kV, and

multi infeed configuration required a pilot wire distance protection to avoid any delay or mal-tripping. From the network shown in Fig. 2, the line sections between G₁ and G₂ (section 7-8 and section 8-9) with their 1st zones boundary plot and overlapping rejoin are indicated in Fig. 5. It can be noticed that the pilot wire distance relays (R₁, R₂, R₃, R₄) are installed at the terminals of each section.

As in Fig. 5, it can be noticed that, 60% from the protected line sections 7-8 and section 8-9 is simultaneously trip by both local and remote terminal relays (R₁ and R₂) and (R₃, R₄) respectively (show the gray regions that represent the overlapping area between Z₁), and the remaining 20% at the boundaries of each section, will be trip instantaneous by its locally relay. For line section 7-8, if the relay R₁ could obtain the response of relay R₂ (by communication channels) for any fault, then the uncertainty in locating faults close to boundary is no more significant and it can quickly clear the fault anywhere on the primary line. For section 7-8, the operating circles for the three zones at bus 7 (solid line) and at bus 8 (broken line), are plotted on the R-X diagrams in Fig. 6. The loading rejoin for each relay are also plotted.

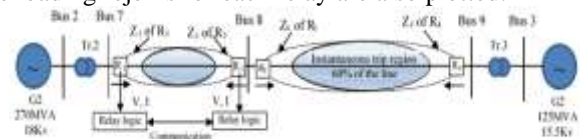


Fig.5 60% from the protected line is fully covered by Z₁.

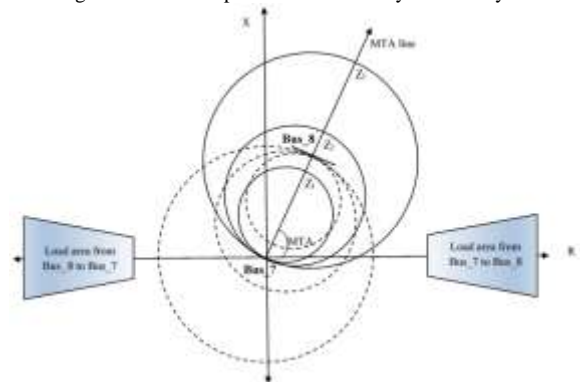


Fig.6 Load area w.r.t Mho distance relay zones for section 7-8.

V. SIMULATION AND RESULTS

In the next sections, fault analysis study is carried out to investigate the performance of pilot distance relays installed on all sections of IEEE 9-Bus network.

VI. FAULT RESISTANCE AFFECT

From the problems that strongly affect the distance relay sensitivity and cause under-reaching of the distance relay is the fault resistance R_f . As explained in [15], the fault impedance seen by the relay (Z_m) for a resistive fault case is not equal to $Z_m = Z_L + R_f$, where (Z_L is the line impedance between the relaying point and the fault point). The error is due to the current infeed from the remote source, which is not seen by the relay. The measured impedance is greater than

this value with amount depending on the ratio between the current infeed from the remote end, and the current seen by the relay. Hence, the impact of fault resistance is manifested clearly with the fault location approaching to the remote end of the relay.

As IEEE 9-Bus system is a multi infeed network, so the effects of the fault resistance will be significantly and should be tested. For the network illustrated in Fig.2, AG fault with fault resistance ($R_f=2\Omega$) at the mid-point of line section 8-9 is simulated. The locus of R_3 and R_4 that are plotted on the same R-X plane is indicated in Fig. 7. It can be seen that, the fault is detected by Z_1 of R_3 and R_4 perfectly, and the fault is tripped instantaneously.

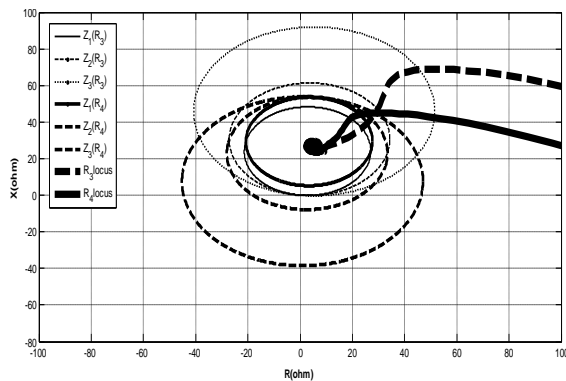


Fig.7 Relys R_3 and R_4 response for AG fault at mid-line of section 8-9 and $R_f=2\Omega$.

Fig. 8 shows the responses of R_1 to R_4 for the same fault with $R_f=15\Omega$. It can be noticed that, the local end relay R_4 is still detecting the fault correctly with its first zone Z_1 . While, R_3 will see the fault in its second zone Z_2 . The difference between the R_3 and R_4 responses is due to the variation of the fault current penetration from G_2 and G_3 that is strongly affected by the distances between the relay location and the generating point. In this case the effect of the multi infeed and fault resistance is manifested.

By increasing the fault resistance, the relays sensitivity is reduced and the remote relay reach will be violated, i.e. the relays will be under-reached. Fig. 9 summarizes the response of the relays R_1 to R_4 for AG fault at midline with $R_f=25\Omega$. It can be noticed that, R_4 locus will settle down at Z_1 boundary, while R_3 will settle down at Z_3 . Also, the relay R_1 at the local end of section 7-8 will fail to provide a backup protection for this fault case.

For this value of fault resistance, whenever, the fault location goes towards R_4 (AG fault at 10Km from bus 9) the sensitivity of the upstream relays (R_1 , R_3) will be completely lost as in Fig. 10. This is due to the fault current infeed from the G_3 terminal is increased when the fault location approach R_4 , this current value is not seen by R_3 and R_1 . The relay R_1 is failed to provide a backup protection for this fault case. From these results, to maintain the relays sensitivity and the system security, the fault resistance value should be less than 25Ω with sufficient amount.

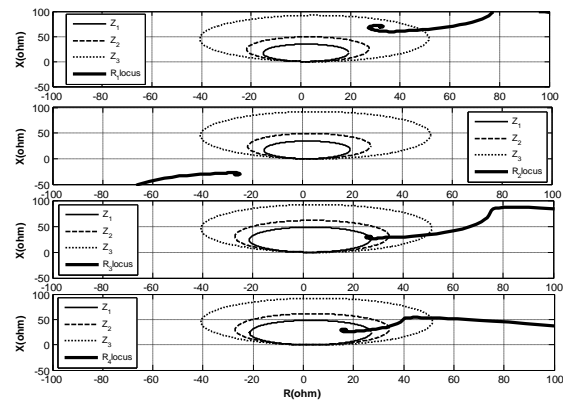


Fig.8 R_1 , R_2 , R_3 and R_4 responses for AG fault at mid-line from Bus 9 of section 8-9 and $R_f=15\Omega$.

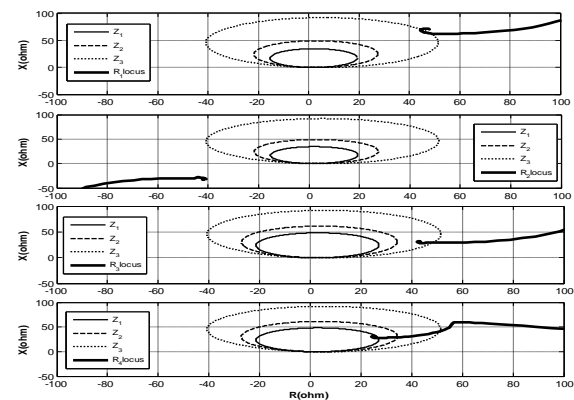


Fig.9 R_1 , R_2 , R_3 and R_4 responses for AG fault at mid-line from Bus 9 of section 8-9 and $R_f=25\Omega$.

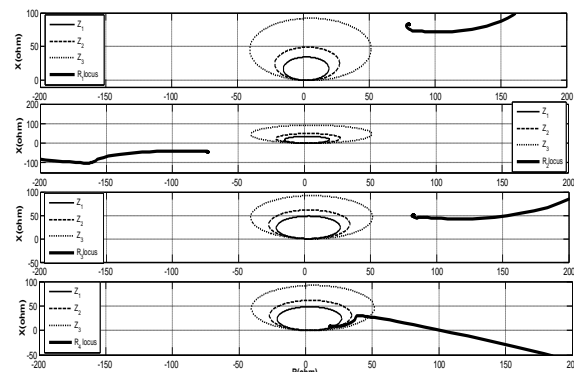


Fig. 10 R_1 , R_2 , R_3 and R_4 responses for AG fault at 10Km from Bus 9 of section 8-9 and $R_f=25\Omega$.

By decreasing the value of the fault resistance from 25Ω to 10Ω , the performance of the relays (R_1 , R_2 , R_3 , R_4) is improved the fault is tripped instantaneously by Z_1 of R_4 , and R_1 provide a backup protection by its Z_3 . Notice that, the fault is detected by the predicted zone for R_1 and R_4 while R_3 is underreached as in Fig. 11. Z_1 for relay R_3 is failed to trip the same fault at 96Km (90.0%) from Bus 9 for section 8-9 and $R_f=20\Omega$, due to the infeed current from G_2 , but it could be detected by its Z_2 , and tripped after T_2 time delay as in Fig. 12. In case of using traditional step distance relay without

communications, this fault is detected by Z_3 for relay R_4 . So, using of pilot distance relay increase the system security and fault resistance converges for the boundary faults.

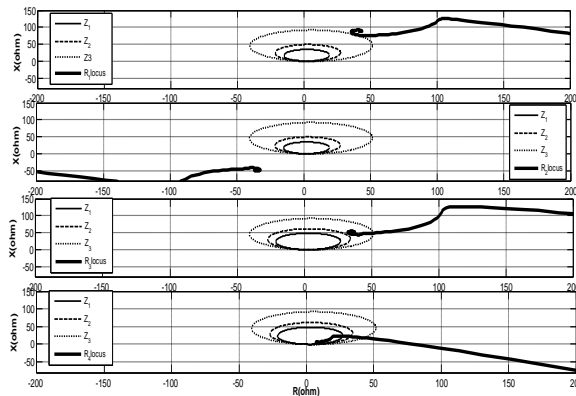


Fig. 11 R_1, R_2, R_3 and R_4 responses for AG fault at 10Km from Bus 9 of section 8-9 and $R_f=10\Omega$.

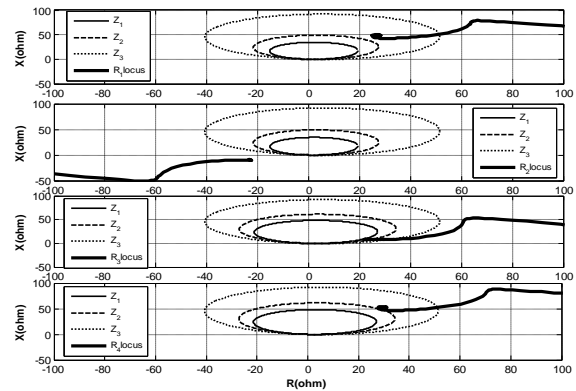


Fig. 12 R_1, R_2, R_3 and R_4 responses for AG fault at 96Km (90.0%) from Bus 9 for section 8-9 and $R_f=20\Omega$.

For BG fault at 70Km (92%) from Bus 7 for section 7-8 with $R_f=5\Omega$, it can be noticed the fault is seen by Z_1 for the relay R_2 , as in Fig. 13. All the relays locus is settling down on the predicted zones due to the small value of the fault resistance. Here, the fault tripping has been accelerated by using signaling based relay, i.e. in the case of using the non-pilot distance relay, this fault is tripped with delay time of Z_2 .

Increasing the fault resistance value to 10Ω , the same responses of all relays are obtained as in Fig. 14. The pilot relay provides the instantaneous tripping for the resistive ground faults at the remote end boundary with fault resistance equal 10Ω . On the other hand, when the fault resistance increases to 15Ω , the fault could not be trip instantaneously by any one of the relays. As in Fig. 15, the fault is seen by Z_2 for the relay R_2 , and Z_2 for the relay R_1 , and Z_3 for the relay R_4 .

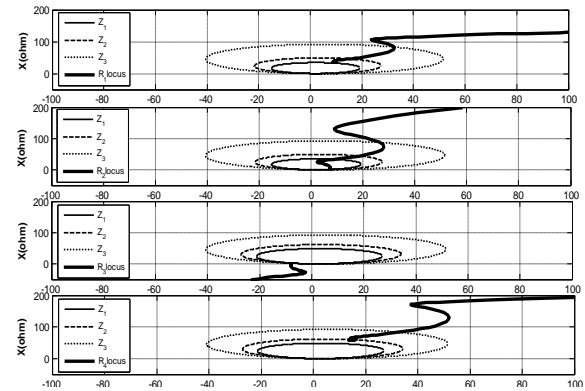


Fig. 13 R_1, R_2, R_3 and R_4 responses for BG fault at 70Km from Bus 7 for section 7-8 and $R_f=5\Omega$.

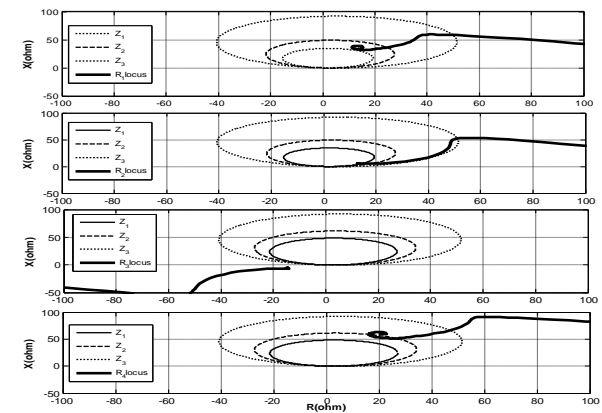


Fig. 14 R_1, R_2, R_3 and R_4 responses for AG fault at 70Km from Bus 7 for section 7-8 and $R_f=10\Omega$.

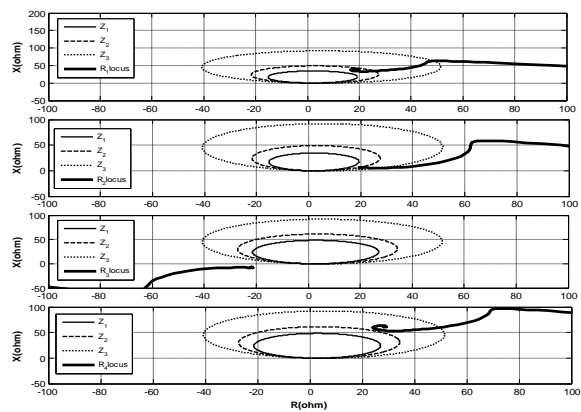


Fig. 15 R_1, R_2, R_3 and R_4 responses for AG fault at 70Km from Bus 7 for section 7-8 and $R_f=15\Omega$.

From the above discussion, it can be concluded that, the Mho distance relay ability to detect the resistive ground fault is depending on some factors such as :-

- 1) The fault location with respect to the relay location. The closer the fault location is to the relaying point, the more chances for the faults to be detected by the relay 1st zone.

- 2) The relay location w.r.t the generating point. The closer the relay location from the feeding point, the more chance for fault detection in its 1st zone (R_1 and R_4).
- 3) The fault location w.r.t. the remote infeed. The closer the fault location to the remote infeed point, the less chances for the fault to be detected in the 1st zone of the relay [R_2 and R_3].
- 4) The multi sections transmission line lengths in the multi infeed network. The sectionlength affects the fault current infeed seen by the relay in the next section, hence affects the measured impedance seen by the relay.
- 5) The value of the fault resistance. The larger the fault resistance, the more chances for the distance relay to under-reach and provide a delayed trip order.

The relays performances for line-to line, line-to-line-to ground, and three phase faults are also tested. For solid AB fault at 70Km (92%) from Bus 7, the fault detected by Z_1 for relay R_2 as in Fig. 16. Also, the performance of the relays for ABG fault at 60% from Bus 7 with $R_f=10\Omega$ is accurate as shown in Fig. 17. The fault detected by Z_1 for the relays R_1 & R_2 and by Z_3 for the relay R_4 . The relays responses for three phase faults (solid ABC fault at 80Km (75%) from Bus 9 is indicated on Fig. 18. It can be noticed that the fault could be detected accurately by Z_1 for the relays R_3 & R_4 and by Z_3 for the relay R_1 .

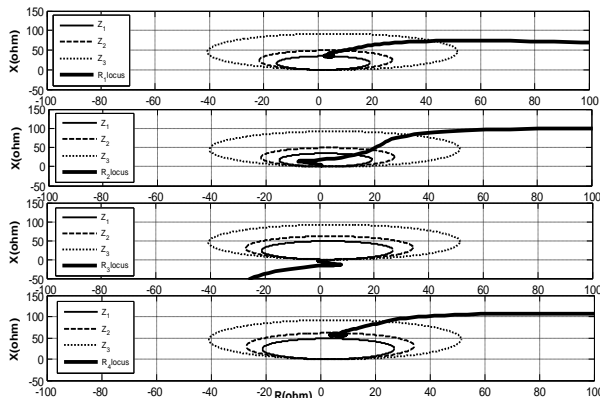


Fig. 16 R_1, R_2, R_3 and R_4 responses for AB fault at 70Km (92%) from Bus 7 for section 7-8 and $R_f=0\Omega$.

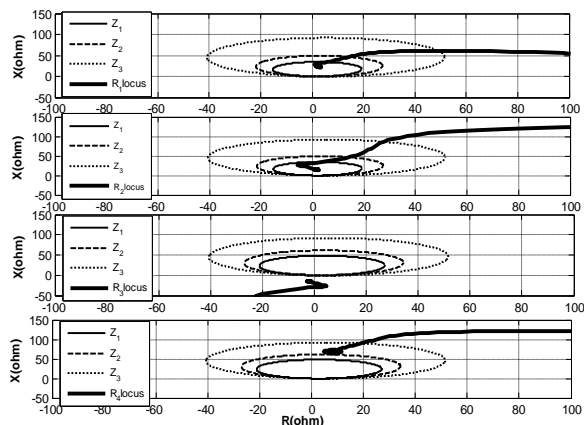


Fig. 17 R_1, R_2, R_3 and R_4 responses for ABG fault at 46Km (60%) from Bus 7 for section 7-8 and $R_f=10\Omega$.

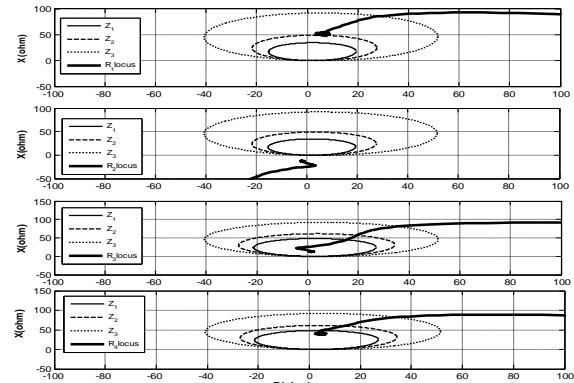


Fig. 18 R_1, R_2, R_3 and R_4 responses for solid ABC fault at 80Km (75%) from Bus 9 for section 8-9.

VII. MAXIMUM TORQUE ANGLE (MTA) AFFECT

The problem of fault resistance to malfunctions of distance protection represents a sustainable problem, many publications have tried to provide a solution for it by modifying the relay reach. By including the effect of remote infeed and arc resistance in the zone's settings calculations, the author in [16] try to overcome the fault resistance effect. Also, by modifying the mathematical core for locating earth faults, a new formula independent of the fault impedance is presented in [17]. However, it is difficult to be incorporated in the distance protection due to the necessity of fast calculation and the unavailability of pre-fault data.

By decreasing the value of the MTA to a value equal 60° and increasing the first and second zones reaches (Z_1 and Z_2) to a value equal to (90% and 150%), the relays response is enhanced for the resistive ground fault. For the same fault shown in Fig. 11 and the relays R_1 and R_2 could detect the fault accurately by its first and second zone respectively as in Fig. 19. Comparing with Fig. 12, the locus of relay R_3 will settle down at its Z_1 as in Fig. 20. Obviously, the relay characteristic deviation toward the load region will enhance the resistive fault converge. On the other hand, decreasing MTA of Z_3 will cause its axis to incline toward the load area, hence the chance of mal-operation of Z_3 due to sudden load change. To avoid that, the MTA of Z_3 should be not decreased.

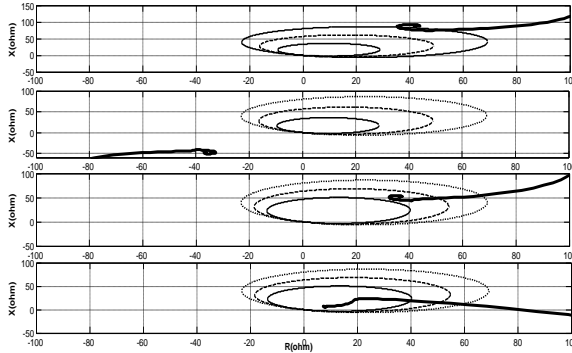


Fig. 19 R_1, R_2, R_3 and R_4 responses for AG fault at 10Km from Bus 9 of section 8-9 and $R_f=10\Omega$ and $MTA=60^\circ$, and Z_1 reach is 90%, Z_2 reach is 150%.

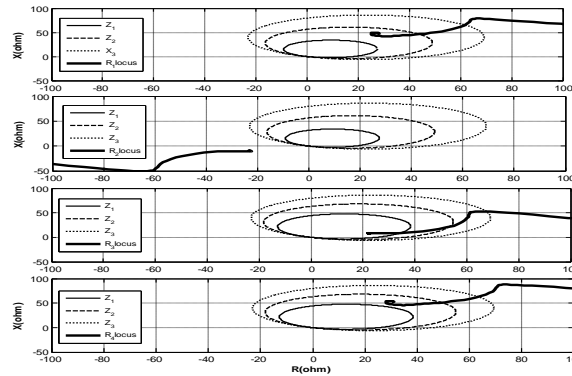


Fig. 20 R_1, R_2, R_3 and R_4 responses for AG fault at 96Km (90%) from Bus 9 of section 8-9 and $R_f=20\Omega$ and $MTA=60^\circ$, and Z_1 reach is 90%, Z_2 reach is 150%.

VIII. MAXIMUM LOADABILITY LIMIT

For Mho distance relay, the zone of protection with greater risk is Z_3 , since its circle with the greatest area and closest proximity to the load impedance. Z_3 settings are certainly vulnerable to load encroachment conditions during high load and power swings conditions, which can cause the load impedance to travel towards the boundaries of the Z_3 Mho circle and cause an undesired trip[13]. the minimum loadability limit for distance relay is given by:

$$MVAT = \frac{(0.85V_{LL})^2}{Z_r * \cos(MTA - \varphi)} \quad (1)$$

Where,

- MVAT → Minimum MVA required to trip.
- VLL → Nominal line voltage in kV.
- MTA → Maximum Torque Angle of relay.
- Z_r → Relay reach in primary Ohms at MTA.
- φ → Maximum anticipated phase angle of load.

By increasing the load at substation 8, by the value equal the loadability limit of the line section 7-8, it can be noticed that the locus of R_1 will enter to its Z_3 circle and the relay will provide a mal-tripping order as in Fig. 21. By increasing the relays MTAs to 90° , the Z_3 circle is slightly deviated

away from the loading area and the security of the relay is enhanced as in Fig. 22.

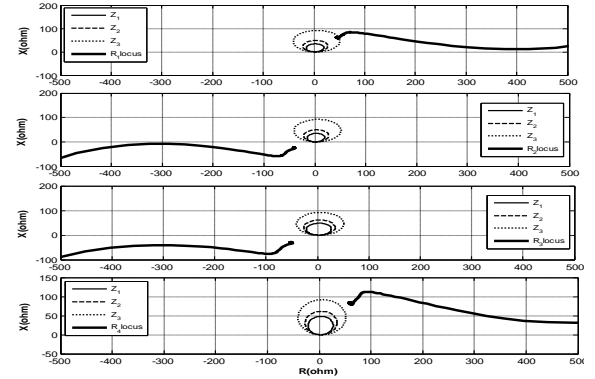


Fig. 21 R_1, R_2, R_3 and R_4 responses for sudden increase of load with value equal the minimum loadability limit at the load center 1 (Load1) at Bus 8.

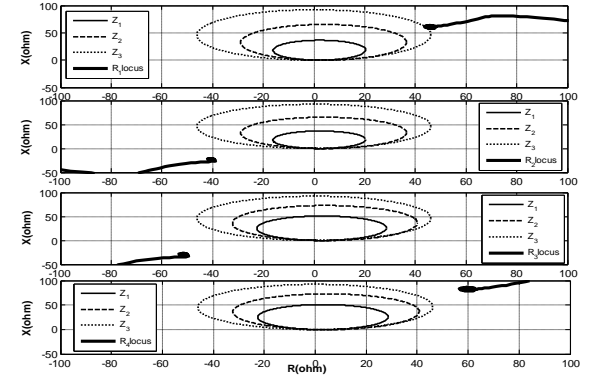


Fig. 22 R_1, R_2, R_3 and R_4 responses for sudden increase of load with value equal the minimum loadability limit at the load center 1 (Load1) at Bus 8 for MTA of Z_3 equal 90° .

IX. CONCLUSIONS

Under different loading and fault conditions of the transmission line, the signaling based-Mho distance relay performances is investigated. In this paper, a deeply fault analysis study for different line sections of IEEE 9-Bus system has been carried out to test the relay performances.

The fault tripping at the remote ends boundaries is accelerating using a pilot scheme, also the relay sensitivity for the resistive ground faults is enhanced. The resistive ground fault converges is increased by increasing the relay reach as well as decreasing the relay MTA. However, the relay sensitivity is increased by decreasing the relay MTA, the relay security during heavy loaded and swing conditions is decreasing. To compromise between the relay sensitivity and its security, the relay MTA of Z_3 should be selected carefully to avoid the load encroachment during the system swings.

X. REFERENCES

- [1] A. D. Zahran, N. I. Elkalashy, M. A. Elsadd, T. A. Kawady and A. I. Taalab, "Improved ground distance protection for cascaded overhead-submarine cable transmission system," 2017 Nineteenth International Middle East Power Systems Conference (MEPCON), Cairo, 2017, pp. 778-758. doi:10.1109/MEPCON.2017.8301269

- [2] J. Lewis Blackburn, Thomas J. Domin, "Protective relaying principles and applications", 3rd Edition.
- [3] P.M. Anderson, "Power System Protection ", IEEE Order No. PC5389, McGraw-Hill, ©1999. 1300 pages of insight.
- [4] DONG Xin-zhou, CAO Run-bin, WANG Bin, SHI Shen-xing, Dominik Bak, "India blackout and three functions of protective relay", Published 2013 Power System Protection and Control, CNKI.
- [5] Hassan Haes Alhelou¹, Mohamad Esmail Hamedani-Golshan, Takawira Cuthbert Njenda¹ and Pierluigi Siano, "A Survey on Power System Blackout and Cascading Events: Research Motivations and Challenges", MDPI, Energies 2019,12.
- [6] S. H. Horowitz, A. G. Phadke, "Third Zone Revisited", IEEE transactions on power delivery, Vol. 21, No. 1, January 2006.
- [7] G. Kobet et al., "Justifying pilot protection on transmission lines," 2010 63rd Annual Conference for Protective Relay Engineers, College Station, TX, 2010, pp. 1-31, doi: 10.1109/CPRE.2010.5469497.
- [8] Kenneth C. Behrendt, "Relay-to-Relay Digital Logic Communication for Line Protection, Monitoring, and Control", 32nd Annual Minnesota Power Systems Conference, October 1996.
- [9] IEEE 9-Bus modified test system data sheet, available online on https://www.ademia.edu/30856140/IEEE_9_BUS_MODIFIED_TEST_SYSTEM_DATA_Nomenclature.
- [10] M. Kiruthika and S. Bindu, "Performance Analysis of a Distance Relay for Zone Identification," 2018 2nd IEEE International Conference on Power Electronics, Intelligent Control and Energy Systems (ICPEICES), Delhi, India, 2018, pp. 206-211, doi: 10.1109/ICPEICES.2018.8897426.
- [11] J. N. Rai, A. Jahangir and I. Hoque, "Digital simulation of distance relay for long transmission line," 2017 4th IEEE Uttar Pradesh Section International Conference on Electrical, Computer and Electronics (UPCON), Mathura, 2017, pp. 91-96, doi: 10.1109/UPCON.2017.8251028.
- [12] A. A. H. Mohamad and E. G. Ahmed, "MATLAB-Simulink S-Function for modeling a digital MHO distance relay," 2015 International Conference on Computing, Control, Networking, Electronics and Embedded Systems Engineering (ICCNEEE), Khartoum, 2015, pp. 230-235, doi: 10.1109/ICCNEEE.2015.7381368.
- [13] Mohamed A. Badr, Nabil H. Abassy Emtethal and N. Abdallah, "Simulation of Distance Relay for Load Encroachment Alleviation with Agent Based Supervision of Zone-3". Renewable Energy and Sustainable Development (RES D) Volume 3 Issue 1, Special Issue, March 2017 - ISSN 2356-8569.
- [14] A. M. Tsimsios and V. C. Nikolaidis, "Setting Zero-Sequence Compensation Factor in Distance Relays Protecting Distribution Systems," in IEEE Transactions on Power Delivery, vol. 33, no. 3, pp. 1236-1246, June 2018, doi: 10.1109/TPWRD.2017.2762465.
- [15] M. E. Erezzaghi and P. A. Crossley, "The effect of high resistance faults on a distance relay," 2003 IEEE Power Engineering Society General Meeting (IEEE Cat. No.03CH37491), Toronto, Ont., 2003, pp. 2128-2133 Vol. 4, doi: 10.1109/PES.2003.1270943.
- [16] Irshad Ulla¹, M S Radwan¹, MNR Baharom¹, H. Ahmad¹, H.M. Luqman¹, Zainab Zainal¹, "Remote Infeed and Arc Resistance Effects on Distance Relays Settings for 9 Bus Wsc System". Advances in Electrical and Electronic Engineering: From Theory to Applications AIP Conf. Proc. 1883, 020047-1–020047-11; doi: 10.1063/1.5002065.
- [17] Elsadd, M. A., Elkalashy, N. I., Kawady, T. A., and Taalab, A.-M. I. (2016), Earth fault location determination independent of fault impedance for distribution networks, Int Trans Electr Energ Syst, doi: 10.1002/etep.2307.